Stochastic Emulation with Enhanced Partial Replication Strategy for Seismic Response Estimation

Sang-ri Yi
Postdoctoral Researcher, Dept. of Civil and Environmental Engineering, University of California, Berkeley, USA

Alexandros Taflanidis
Professor, Dept. of Civil and Environmental Engineering and Earth Sciences, University of Notre Dame, Notre Dame, USA

ABSTRACT: Modern performance-based earthquake engineering practices typically entail a large number of time-consuming nonlinear time history simulations to appropriately incorporate excitation and model uncertainties in the decision making process. Surrogate modeling techniques have emerged as attractive tool for alleviating this computational burden, while allowing for the use of high-fidelity numerical models to describe hysteretic structural response. A key challenge arises in this setting for accurately capturing the aleatoric uncertainty associated with the seismic hazard. This uncertainty is typically expressed as high-dimensional or non-parametric uncertainty (depending on the approach adopted for modeling ground motion time histories), and so cannot be easily incorporated within standard surrogate modeling frameworks. Recent work has shown how stochastic emulation techniques can be leveraged to address this challenge, utilizing Gaussian Process regression (GP) as foundational surrogate model technique. Established formulation requires, for some of the parametric configurations examined, the replication of the simulations to capture the aleatoric response variability. The simulations with replications are leveraged to inform a secondary GP to describe the heteroscedastic aleatoric variability, whereas all simulations and the secondary GP are then used to establish a primary GP for predicting the response distribution. This formulation has two challenges: (i) it requires replications for some of the configurations; (ii) it only uses the configurations with replications to inform the secondary GP development. Here, an enhancement is proposed to address both these challenges: a GP-based approximation is first established for the median response, and leveraging this approximation, all simulations are utilized for developing the secondary GP. Case study examples demonstrate the benefits of the alternative formulation and the fact that it addresses both aforementioned challenges.

1. INTRODUCTION

Decision making for earthquake engineering applications requires proper consideration of various type of uncertainties for the seismic hazard and the infrastructure models. Accurate assessment of risk in this context entails a large number of simulations (nonlinear time-history analyses) of complex numerical models (representing the infrastructure), creating a large computational burden. One attractive approach to alleviate such computational burden is to replace the expensive numerical model with a surrogate model developed using a small number of judicially chosen simulations, frequently also referenced as computer experiments. This surrogate model ultimately establishes an approximate mapping between inputs (i.e. the parameters of earthquake and structural models) and outputs of interest (structural responses), and can significantly accelerate risk assessment.

The aleatoric uncertainty associated with the seismic hazard, stemming from the complex physical mechanism of earthquake generation and propagation, creates significant challenges in such surrogate modeling applications. Often only a

limited number of parameters are used to describe phenomenological causality, and the portion of uncaptured uncertainty is described as aleatory uncertainty, propagated to the model outputs as requirement to estimate the distribution of the responses (under this uncertainty). To properly describe such stochasticity in responses, specially designed surrogate modeling techniques have been devised, often referred to as stochastic emulators (Ankenman *et al.* 2010, Binois et al 2018). A branch of such approach quantifies the output uncertainty by deliberately generating so-called "replications" which refers to multiple simulation response realizations for identical input parameters. The variance estimate obtained by the replications help to directly estimate the variance in the response serving as the *samples* of a heteroskedastic variance field. Although, it was shown in the literature (Binois *et al*. 2018; Wang and Haaland 2018) that replications are an effective way of disaggregating the heteroskedastic variance component from the simulation results, it naturally demands higher computational cost.

To mitigate some of the computational burden of creating replications recent research efforts (Kyprioti and Taflanidis, 2021; Kyprioti and Taflanidis, 2022) investigated partial replication strategies, formulating a framework which incorporates both replicated and non-replicated simulation experiments. In this approach, the replicated samples are used to obtain variance estimates at the sampled locations, and these estimates are used to construct a continuous mapping of a variance-field across the sample space. Then one can constrain the relative scales of the variance to train the primary emulator, exploiting both replicated and non-replicated samples. One drawback of this approach is that only a fraction of the samples is utilized when constructing the variance-field because non-replicated samples solely cannot provide any information on the response variance, and that it requires a minimal number of replications to be considered.

This work proposes a practical extension of the prescribed partial replication strategy that addressed both aforementioned challenges. In particular, previous works that investigated seismic response emulators suggest that even when high heteroskedasticity exists for the aleatoric uncertainty, mean-field prediction is quite robust to the choice of the variance model (Kyprioti and Taflanidis, 2021). Motivated by this, we establish a preliminary, primitive mean-field approximation through a homoscedastic stochastic emulator. Instead of using replication-based samples, the variance-field mapping is informed by the deviation of the simulations from the mean response approximation (Marrel et al. 2012). This way, the information of unique samples can be fully utilized not only in the mean-field predictions but also in the variance-field predictions. The framework can also be implemented without considering any replications, allowing the available computational budget to be used for better exploration of the parametric domain. In the presented numerical examples, the proposed method shows excellent performance in capturing the underlying heteroskedastic trend compared to the considered alternatives with the same training sample size.

2. PROBLEM FORMULATION

Let us consider a joint model for describing ground motion excitation and structural response. In the presentation, a stochastic ground motion model will be used for the excitation, though ideas can be extended to any desired approach for describing seismic hazard. The ground motion model entails two types of uncertainty. The first type pertains to key ground motion features, for example related to intensity, seismicity properties or excitation characteristics (duration, frequency content). This uncertainty source can be described by a parametric formulation, with corresponding variables denoted herein by $\mathbf{x}_g$. The second type pertains to aleatoric variability of the excitation, frequently referenced as ground-motion to ground-motion variability. Depending on the excitation model, this uncertainty source might not have a parametric description (corresponds to latent features of the excitation model), or might correspond to a high-dimensional stochastic

sequence **w**, when stochastic ground motion models are utilized for describing the seismic hazard (Kyprioti and Taflanidis, 2022). Additionally, the structural model might entail its own parameters, described by random variable vector $\mathbf{x}_s$. We will denote by $\mathbf{x}=[\mathbf{x}_s, \mathbf{x}_g]$ the vector of model parameters for the joint excitation and structural models. Objective of the stochastic emulation is to approximate the distribution of the structural response, denoted z herein, as function of **x** while considering the influence of the aleatoric hazard variability.

Adopting kriging as stochastic emulation strategy, this is ultimately accomplished by approximating $z(\mathbf{x})\sim N(m(\mathbf{x}),\sigma^2(\mathbf{x}))$, where $N(.,.)$ stands for Gaussian distribution and $m(\mathbf{x})$ and $\sigma^2(\mathbf{x})$ represent, respectively, the predictive mean and variance of the surrogate model. In this context, kriging emulation approximates the response as a realization of a Gaussian process (GP), utilizing formulation $z(\mathbf{x})=y(\mathbf{x})+\varepsilon(\mathbf{x})$, where $y(\mathbf{x})$ is a GP with some chosen mean trend [typically expressed as a linear regression combining basis vector $\mathbf{f}(\mathbf{x})$ and coefficients $\boldsymbol{\beta}$], and a stationary correlation kernel (Williams and Rasmussen 2006), and $\varepsilon(\mathbf{x})$ is the so-called nugget parameter, assumed to follow a zero mean Gaussian distribution with variance $\tau^2(\mathbf{x})$. This nugget is the component leveraged to address the aleatoric uncertainties in the problem formulation (Kyprioti and Taflanidis, 2021). When the nugget variance is constant, the problem reduces to a simpler homoscedastic case, though it has been shown (Kyprioti and Taflanidis, 2021) that this is a poor approximation for describing nonlinear structural response. The emphasis is herein on how to address a heteroscedastic nugget.

3. REVIEW OF STOCHASTIC EMULATION WITH PARTIAL REPLICATION

This section briefly reviews the stochastic emulation with partially replicated samples (Kyprioti and Taflanidis 2021). This approach leverages two GP models: the primary one with heteroscedastic nugget approximates the response $z(\mathbf{x})$, while its nugget variance $\tau^2(\mathbf{x})$ is approximated by the secondary GP.

To formalize implementation, consider N_p training points that are replicated n_p times, referred to as *replicated points* and additional N_s training points which are not replicated, denoted as *non-replication points*. In such setting, a total of $N_t=N_s+N_pn_p$ high-fidelity simulations are involved in this surrogate model training. The replications pertain to different samples (different realizations) for the aleatoric sources of uncertainty, for example to different stochastic sequences when stochastic ground motion model is used for the excitation. Superscript i will be used to denote the ith parametric configuration and notation $z^{i,j}$ will be used to describe the j-th response realization for the training points with replications. For the latter points we can obtain the unbiased estimates for the mean and the variance, respectively, as

$$\bar{z}^i=\frac{1}{n_p}\sum_{j=1}^{n_p} z^{i,j} \tag{1}$$

$$(\tau^2)^i=\frac{1}{n_p-1}\sum_{j=1}^{n_p}(z^{i,j}-\bar{z}^i)^2 \tag{2}$$

Using the results from Eq. (2) as observations, a secondary GP is first established to predict the continuous field of the response variance. Assuming homoscedasticity for this GP, any traditional calibration and prediction formulations can be adopted (Williams and Rasmussen 2006). Note that the homoscedastic nugget in this auxiliary GP accounts for the variability in the obtained sample variances of Eq. (2) [sample-based estimation error].

Once the variance field is estimated, the final predictive mean and variance can be estimated using information for both the replicated samples, $\mathbf{x}^i$ and $\bar{z}^i$ (i=1,…,N_p), and the non-replicated samples, $\mathbf{x}^i$ and z^i (i=1+N_p,…,N_s+N_p), as:

$$m(\mathbf{x})=\mathbf{f}(\mathbf{x})^T\boldsymbol{\beta}+\mathbf{r}(\mathbf{x})^T\tilde{\mathbf{R}}^{-1}(\mathbf{Z}-\mathbf{F}\boldsymbol{\beta}) \tag{3}$$

$$\sigma^2(\mathbf{x})=\tau^2(\mathbf{x})+\tilde{\sigma}^2[1+\boldsymbol{\gamma}(\mathbf{x})^{\mathrm{T}}\{\mathbf{F}^{\mathrm{T}}\tilde{\mathbf{R}}^{-1}\mathbf{F}\}^{-1}\boldsymbol{\gamma}(\mathbf{x})-\mathbf{r}(\mathbf{x})^{\mathrm{T}}\tilde{\mathbf{R}}^{-1}\mathbf{r}(\mathbf{x})] \tag{4}$$

where $\tilde{\mathbf{R}}=\mathbf{R}+\delta_s\mathbf{A}^{-1}\tilde{\mathbf{C}}_s$, $\boldsymbol{\beta}=(\mathbf{F}^{\mathrm{T}}\tilde{\mathbf{R}}^{-1}\mathbf{F})^{-1}\mathbf{F}^{\mathrm{T}}\tilde{\mathbf{R}}^{-1}\mathbf{Z}$, $\boldsymbol{\gamma}(\mathbf{x})=\mathbf{F}^{\mathrm{T}}\tilde{\mathbf{R}}^{-1}\mathbf{r}(\mathbf{x})-\mathbf{f}(\mathbf{x})$, $\tilde{\mathbf{C}}_s$ is a diagonal matrix of with elements $\tau^2(\mathbf{x}^i)$, and **A** is a diagonal matrix

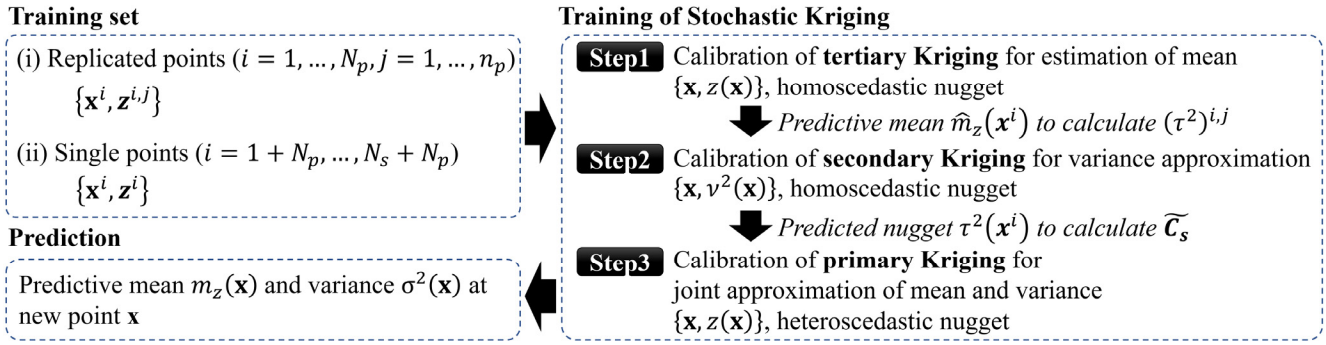

Figure 1: Procedure of the stochastic kriging

with elements n_i which represents the replication size at i-th unique training points, i.e. either n_p or 1. **F** and **Z** are the matrices whose i-th row is respectively $\mathbf{f}(\mathbf{x}^i)$ (the basis functions for the underlying GP regression) and $\bar{z}^i$ (for points with replications) or z^i (for points without replications). The scalar quantity $\tilde{\sigma}^2$ is the process variance and δ_s is the nugget scaling parameter. The GP calibration can be done by maximum likelihood estimation, with details included in (Kyprioti and Taflanidis, 2021).

Drawbacks of this approach is that replications are always needed and that the non-replication points are not fully utilized when estimating the variance field. The trade-off between the number of point with and without replication, and the number of replications examined per points has been investigated in detail in the numerical experiments performed in Kyprioti and Taflanidis (2021), showing that the overall accuracy improves as more non-replication points are utilized, with a considerable reduction of performance, though, as the number gets close to N_t. This performance reduction is largely attributed to the limited information available for the development of the variance-field (secondary GP), since non-replication points cannot be used for this development.

4. ENHANCED PARTIAL REPLICATION APPROACH

An enhanced version of the stochastic emulation framework [also shown in Figure 1] is described here, with objective to utilize all points (even the non-replication points) for the variance-field approximation is proposed in this Section. Unlike the previous approach which relied on the pure sample variance [given by Eq. (2)] to construct the secondary GP, the proposed method introduces tertiary GP model for a quick estimation of the underlying mean function, which can be leveraged to obtain samples of the variance from single observations. In particular, this mean function is first obtained by fitting a traditional homoscedastic kriging model, i.e. assuming the nugget variance $\tau^2(\mathbf{x})$ is a constant, to the entire training dataset. Similar to the secondary GP discussed in the previous section, any standard formulation (Williams and Rasmussen 2006) can be adopted for the tertiary GP. Let us denote the predictive mean acquired by this as $\hat{m}_z(\mathbf{x})$. Then for both the non-replicated and replicated points, an estimation of the sample deviation from the mean can be obtained as:

$$(\tau^2)^{i,j} = \left(z^{i,j} - \hat{m}_z(\mathbf{x}^i)\right)^2, \quad j = 1,...,n_i \tag{5}$$

where i=1,…,N_p+N_s.. The sample deviation $(\tau^2)^{i,j}$ by definition can be used as an alternative to Eq. (2) for the variance-field estimation. To account for the fact that for the points with replications, multiple observations are available for the sample deviation from the mean, a partial replication-based formulation [similar to the one given by in Eq. (3) but with a homoscedastic nugget variance] needs to be adopted to establish the mapping between **x** and $\tau^2(\mathbf{x})$ for the secondary GP using dataset $(\tau^2)^{i,j}$. Finally, the process of training the primary GP model is the same, simply the updated secondary GP predictions are utilized.

The major difference between the original and alternative variance estimators, is that while

the original [utilizing Eq. (2) as observations] relies on the pure sample variance, the modified one [utilizing Eq. (5) as observations] treats the mean estimate obtained from the auxiliary GP model as the true mean (population mean) and variance is estimated as the sample deviation from the mean. This difference allows the latter to accommodate the non-replicated samples. This is especially useful when there are only limited replications available, or when the response trend shows localized nonlinearities requiring better space-filling exploration of the domain.

Of course, it should be noted that the proposed method is heuristic in a way that it assumes that the mean estimate obtained from the crude homoscedastic nugget assumption, $\hat{m}_z(\mathbf{x})$, gives a reasonably reliable estimate. This assumption relies on past studies (Kyprioti and Taflanidis, 2021; Kyprioti and Taflanidis, 2022), that have shown that for seismic applications the mean-field prediction is relatively robust to the choice of the variance model, especially compared to the level of variability observed in the sample replications. This was also observed in more general, non-seismic, applications investigated in Marrel et al. (2012).

Furthermore, note that if the final estimation of mean $m_z(\mathbf{x})$ (from Step3 of Figure 1) is significantly different from the initial estimate $\hat{m}_z(\mathbf{x})$ (from Step1), then one may iterate Step 2-3 by replacing $\hat{m}_z(\mathbf{x})$ with the $m_z(\mathbf{x})$ until the two functions become more similar. Note that, as mentioned in Marrel et al. (2012), this iteration is rather heuristic and is not guaranteed to converge.

Table 1 Structural parameters for surrogate training

Notation	Parameter (model)	Range
ζ_s	Rayleigh damping ratio (%)	3-8.2
f_{c1}, f_{c2}, f_c	Compressive strength(c) at each floor (MPa)	17-46.1
$\varepsilon_{c1}, \varepsilon_{c2}, \varepsilon_{c}$	Strain at maximum strength(c) at each floor (MPa)	0.0012-0.0033
E_s	Elastic modulus(s) (GPa)	180-230
f_y	Yield stress(s) (MPa)	430-700
a	Straining hardening ratio(s)	0.006-0.017

* (c): Concrete02, (s): Steel02

Finally note that one limitation from the previous work still applies to the proposed approach: for the secondary and tertiary kriging models, point estimates corresponding to the mean predictions are only used, omitting the uncertainty in these predictions. Incorporating, additionally, this epistemic source of uncertainty could perhaps be beneficial for improving accuracy of estimation.

5. NUMERICAL EXAMPLES

5.1. Model descriptions

The same case-study example as in (Kyprioti and Taflanidis, 2021) is used. The structural model corresponds to a three-story, four-bay benchmark concrete structure modeled in OpenSees (McKenna, 2011), using material models of Concrete02 and Steel02. The fundamental period is 0.57 sec and Rayleigh damping is introduced for 1st and 3rd modes. Ten structural parameters are considered as random variables: Rayleigh damping ratio, six concrete material model parameters, and three steel material model parameters. These structural parameters that constitute $\mathbf{x}_s$ are shown in Table 1. The excitation model corresponds to a point source stochastic ground motion models whose parametric description (i.e. $\mathbf{x}_g$ definition) is based on the magnitude, M, and rupture distance r_{rup}. The ranges considered for them are respectively $M \in [5,8]$ and $r_{rup} \in [3,60]$ (km), respectively. The total number of model parameters for $\mathbf{x}$ is $n_x = 12$ and the surrogate model objective is to describe the distribution for the peak inter-story drifts and peak absolute floor accelerations at each story (n_z = 6 total number of output variables). The proposed stochastic emulation is separately established for each of these outputs.

5.2. Examined cases and validation metrics

The numerical investigation focuses on the comparison of the baseline approach in Section 3 – referred to as original – and the proposed approach that utilizes Eq. (5) to get the estimates of the predictive variance. From the fact that the two approaches both accommodate partial replications, we further investigated the benefit

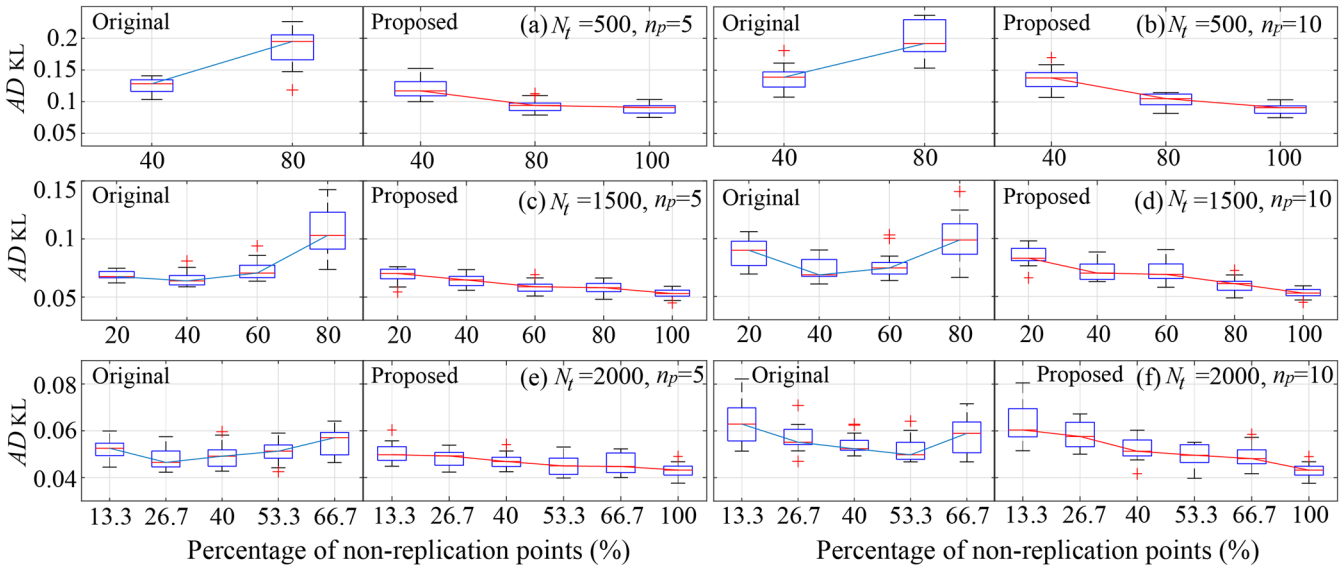

Figure 2: Average KL divergence values. The 'original' refers to Kyprioti and Taflanidis (2021).

offered from replications by exploiting different mixtures of replicated and non-replicated training samples. In particular, two different values of replication size (n_p = 5 and 10) are investigated, as well as the varying numbers of the total samples size (N_t=1500, 1000, and 500). Similarly, chosen cases of N_s are N_s=200, 400, 600, 800, 1000, and 1500. Among the listed N_s and N_t values, the pairs that satisfy N_s<N_t are investigated in the original implementation, and N_s=N_t cases (i.e. no replications) are additionally included for the proposed implementation, as the latter became applicable after introducing the variation in Eq. (5). Note that, for example, when (N_t=1500, N_s=200, n_p=10) is chosen, the number of replicated points was N_p=(N_t-N_s)/n_p=13. Similarly, when (N_t=500, N_s=500) is chosen, regardless of n_p, all the samples in the training sets are non-replication points and N_p is zero.

The surrogate models are validated using total of 200,000 test samples consisting of 1,000 randomly selected test locations across the training domain, each having 200 replications. The Monte Carlo estimates of the mean and variance estimations at the 1,000 test locations are compared with the estimations from the two surrogate models. To evaluate the overall prediction error in the response distribution, Kullback-Leibler (KL) divergence metric which measures the distance between the estimated and reference probability distributions is calculated following the formulation in Kyprioti and Taflanidis (2021). Additionally, the individual performance metrics for the predictive mean and variance are examined by comparing correlations between the prediction and exact test sample mean and variances, respectively. The correlation coefficients would ideally approach to 1, when the surrogate predictions are perfect and abundant test samples are available. To assess the robustness of the surrogate model predictions, the training process is repeated independently 15 times with different random seed – different training sample realizations – and validation statistics are averaged across these repetitions.

5.3. Results and discussions

The test set validation results are presented in Figures 2 and 3. Figure 2 shows the average KL divergence metric – averaged over 6 response quantities – for various examined cases. Each row represents different total training sample sizes and each column represents different replication sizes examined. The *x*-axis is the percentage of non-replication points among total training samples (N_s/N_t ×100). The variability of the validation statistics across the 15 repetitions is presented using box plots. Figure 3 shows the correlation coefficient between predicted and the exact responses. Both median and logarithmic variance

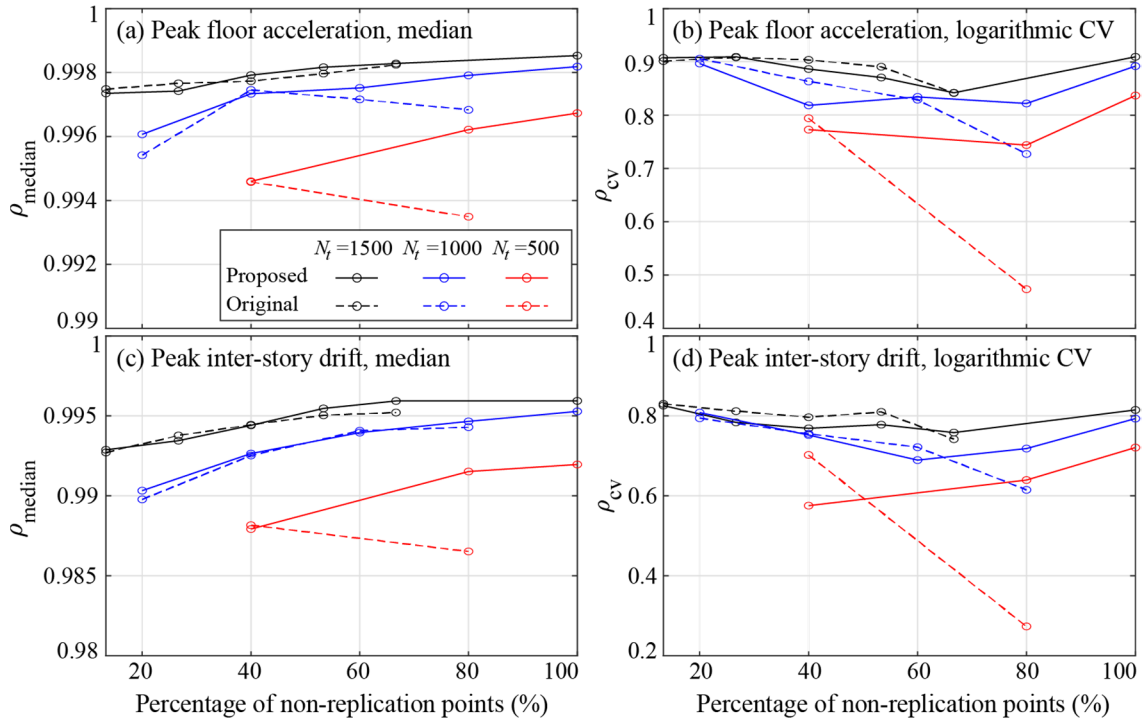

Figure 3: Correlation coefficient metric for median (left) and logarithmic coefficient of variation (right) of the peak floor acceleration (n_p =10, averaged across floors). The 'original' refers to Kyprioti and Taflanidis (2021).

(in terms of coefficient of variation, CV) are examined for different training sample sizes and the proportions of non-replication points. In particular (a) and (b) are the peak floor acceleration prediction results averaged across over different floors and (c) and (d) are those of peak inter-story drift. Only the case of n_p=10 is presented here, but n_p=5 case also showed very similar observations. In this case the average performance across the 15 repetitions is shown.

It can be observed in Figure 2 that as the proportion of non-replication points increases, the error from the proposed method monotonically decreases, reaching below the minimum error of the original approach. This is consistently observed across different training sizes (N_p) and replication sizes (n_p). In particular, when the proportion of the non-replication points is below 50-60%, the performance of the proposed method is similar to the original approach. However, as the percentage gets larger, the error kept decreasing only in the proposed approach, proving that the information from the non-replicated experiments becomes essential in such cases. Furthermore, the proposed approach shows that there is no trade-off between replication and non-replication samples. Rather, consisting of the training set using only the non-replication samples provided the most accurate predictions in the investigated example cases.

Figure 3 further differentiates the error into those in median and CV by introducing the correlation coefficient metric. Furthermore, the correlation coefficients are assessed separately for acceleration and displacement outputs, which demonstrates that the same trend applies to both types of outputs. Looking at the performance of the original approach, one can notice that the prediction accuracy of mean function consistently increases as the percentage of non-replication points increases (shown in (a) and (c)) while that of the variance decays (shown in (b) and (d)). The latter can be explained by the reduction of information on the variance, that is fed into the secondary kriging. However, albeit the decay of variance prediction, exploration offered by non-replication points provides a larger benefit in the mean prediction as evidenced by the increasing trend of the accuracy. Still, the case of 80% non-replication shows that a substantial error in the

variance estimation can actually lead to the poor mean prediction.

For the proposed approach, mean prediction initially follows a similar trend to the original approach, but it continues to increase until it reaches 100% non-replication case. This is explained by non-degraded performance in the variance prediction. The variance performance is similar when the replication points dominate the training samples, suggesting that addition of non-replication points does not benefit in such cases. However, as the proportion of non-replication points increases, they clearly dominate the variance predictions and restore the level of accuracy observed in the heavily replicated cases.

6. CONCLUSION

A new practical stochastic emulation formulation was proposed for earthquake engineering applications. The method advances previous research on the use of a stochastic kriging framework with partial replication. Original framework leverages a secondary Gaussian Process (GP) to estimate the heteroscedastic variability of the primary GP model, with the latter providing the desired approximation for the response distribution. In this setting, among the partially replicated training data, only the portion with replications is utilized for the inference of the variance-field. The proposed enhancement additionally considers the non-replicated sample portion for this objective, by training the secondary GP based on observations of the deviation of non-replication samples from an approximate mean estimate. This mean estimate is obtained leveraging a homoscedastic GP. The proposed method can also be applied to fully non-replicated training sets, utilizing more efficiently the available computational budget for performing numerical simulations (no replications needed).

The case study demonstrated that engagement of non-replication points provides a better overall performance. When the training set consists of large replication points, the performance of the proposed method was similar to the original approach. However, noticeable performance improvement was observed as the proportion of the non-replicated samples increases. The observed findings were consistent across different training sample sizes and replication sizes, while the performance gap was more evident when the training sample size was small. One interesting future research topic would be the adaptive selection of experiments for improving prediction accuracy across both the mean and variance stochastic fields.

7. ACKNOWLEDGEMENTS

This research was financially supported by the National Science Foundation (NSF) under Grant CMMI- 2131111. This support is gratefully acknowledged. Any opinions, findings, and conclusions or recommendations expressed in this material are those of the authors and do not necessarily reflect the views of the NSF.

8. REFERENCES

Ankenman, B., Nelson, B.L., Staum, J. (2010) "Stochastic kriging for simulation meta-modeling" *Operations Research*, 58, 371-382.

Binois, M., Gramacy, R.B., Ludkovski, M. (2018) "Practical heteroscedastic gaussian process modeling for large simulation experiments" *Journal of Computational and Graphical Statistics*. 27(4), 808-821.

Kyprioti, A.P., Taflanidis, A.A. (2021). "Kriging metamodeling for seismic response distribution estimation" *Earthquake Engineering and Structural Dynamics*, 50(13), 3550-3576.

Kyprioti, A.P., Taflanidis, A.A. (2022). "Addressing the different sources of excitation variability in seismic response distribution estimation using kriging metamodeling"*Earthquake Engineering and Structural Dynamics*, 51(10), 2466-2495.

Marrel, A., Iooss, B., Da Veiga, S., Ribatet, M. (2012). "Global sensitivity analysis of stochastic computer models with joint metamodels" *Statistics and Computing,* 22, 833-847.

McKenna F. (2011) "OpenSees: a framework for earthquake engineering simulation" *Computing in Science & Engineering,* 13(4), 58-66.

Wang, W., Haaland, B. (2018). Controlling sources of inaccuracy in stochastic kriging. *Techno-metrics*.

Williams, C. K., Rasmussen, C. E. (2006). "Gaussian processes for machine learning". Cambridge, MA: MIT press.